Apoptin Induces Tumor specific Apoptosis as a Globular Multimer

Leliveld, S.R.; Zhang, Y.-H.; Rohn, J.L.; Noteborn, M.H.M.; Abrahams, J.P.

THE JOURNAL OF BIOLOGICAL CHEMISTRY
Vol. 278, No. 11, Issue of March 14, pp. 9042–9051, 2003
Printed in U.S.A.

Apoptin Induces Tumor-specific Apoptosis as a Globular Multimer*

Received for publication, October 22, 2002, and in revised form, December 18, 2002
Published, JBC Papers in Press, December 19, 2002, DOI 10.1074/jbc.M210803200

Sirik R. Leliveld‡§, Ying-Hui Zhang¶‖, Jennifer L. Rohn¶, Mathieu H. M. Noteborn¶, and Jan Pieter Abrahams‡ ‡‡**

*From the ‡Department of Chemistry, Leiden University, ¶Leadd BV, and **Department of Molecular Cell Biology, Leiden University Medical Center, 2300 RA Leiden, The Netherlands*

The chicken anemia virus-derived Apoptin protein induces tumor-specific apoptosis. Here, we show that recombinant Apoptin protein spontaneously forms noncovalent globular aggregates comprising 30 to 40 subunits *in vitro*. This multimerization is robust and virtually irreversible, and the globular aggregates are also stable in cell extracts, suggesting that they remain intact within the cell. Furthermore, studies of Apoptin expressed in living cells confirm that Apoptin indeed exists in large complexes *in vivo*. We map the structural motifs responsible for multimerization *in vitro* and aggregation *in vivo* to the N-terminal half of the protein. Moreover, we show that covalently fixing the Apoptin monomers within the recombinant protein multimer by internal cross-linking does not affect the biological activity of Apoptin, as these fixed aggregates exhibit similar tumor-specific localization and apoptosis-inducing properties as non-cross-linked Apoptin. Taken together, our results imply that recombinant Apoptin protein is a multimer when inducing apoptosis, and we propose that this multimeric state is an essential feature of its ability to do so. Finally, we determine that Apoptin adopts little, if any, regular secondary structure within the aggregates. This surprising result would classify Apoptin as the first protein for which, rather than the formation of a well defined tertiary and quaternary structure, semi-random aggregation is sufficient for activity.

Apoptin is a protein from chicken anemia virus (CAV)[1] that induces apoptosis in transformed chicken cells (1). It has 121 amino acids and no known functional or sequence homologues. When the gene encoding Apoptin is transduced into cultured cells, the expressed Apoptin protein also induces apoptosis in a wide range of transformed human cell lines (2). However, non-transformed, normal human primary cell types are not killed. Transformed and non-transformed cells differ markedly in the subcellular localization of expressed Apoptin. In transformed cells, Apoptin migrates to the nucleus, whereas in non-transformed cells it is retained mainly within the cytoplasm. Although nuclear localization of Apoptin appears to be essential for apoptosis induction in transformed cells (3), the presence of Apoptin in the nucleus alone is not sufficient to induce apoptosis in normal cells.[2] Two clusters of basic residues (Lys^{82}-Arg^{89}, Arg^{111}-Arg^{120}) near the C terminus of Apoptin have been implicated as a nuclear localization signal.

To correlate Apoptin's biological activity with its structure and biophysical properties, we studied several bacterially expressed, tagged recombinant Apoptin proteins. First, because maltose-binding protein (MBP) fusion constructs can be effective in solubilizing aggregation-prone recombinant proteins, we constructed N-terminally MBP-tagged Apoptin (4, 5). Second, because histidine tagging can allow efficient refolding of protein immobilized on Ni^{2+}-chelating resin (6), we also constructed C-terminally hexahistidine-tagged Apoptin.

MBP-Apoptin fusion constructs were shown to be biologically active and retain their distinct behavior in normal and tumor cells upon microinjection.[3] Here, we addressed Apoptin's biophysical and structural properties and how these relate to its biological function and found it to be biologically active as a higher order multimer. However, no evidence was found for an established regular structure.

MATERIALS AND METHODS

Cloning of Apoptin Expression Vectors (See Table I for the Expressed Constructs)

pET-22bVp3, C-terminal Hexahistidine Fusion of Full-Length Apoptin (Apoptin-H_6)—The Apoptin open reading frame (ORF) was amplified by PCR from pET-11aVp3, which contains the Apoptin coding sequence (nucleotides 427–868 in the CAV genome). The purified PCR fragment was cloned at *Nde*I and *Not*I in pET-22b (Novagen), in which a T7*lac* promoter, inducible with isopropyl-β-D-1-thiogalactoside (IPTG), controls expression.

pET-22bVp3(1–69)H_6, N-terminal 69 Residues of Apoptin with C-terminal Hexahistidine Tag (Apoptin(1–69)-H_6)—The N-terminal domain of Apoptin (ORF nucleotides 1–207) was amplified by PCR and cloned in pET-22b at *Nde*I and *Ava*I.

pMalTBVp3, N-terminal Fusion of MBP and Full-length Apoptin (MBP-Apoptin)—The Apoptin ORF was cloned at 5′ *Bam*HI and 3′ *Sal*I in pMalTB, downstream of the *Escherichia coli Mal*E ORF, which codes for MBP. pMalTB is derived from pMal-c2 (New England Biolabs), and the peptide linker between MBP and its fusion partner contains a thrombin consensus site (-LVPR↓GS-). Expression is controlled by an IPTG-inducible P_{tac} promoter.

pMalTBVp3dC69H_6 MBP Fusion of N-terminal 69 Residues of Apoptin with C-terminal Hexahistidine Tag (MBP-Apoptin(1–69)-H_6)—The truncated Apoptin(1–69) ORF was amplified from pET-22bVp3(1–

* The costs of publication of this article were defrayed in part by the payment of page charges. This article must therefore be hereby marked "*advertisement*" in accordance with 18 U.S.C. Section 1734 solely to indicate this fact.

§ Contributed equally.

‖ Contributed equally.

‡‡ To whom correspondence should be addressed: P. O. Box 9502, 2300 RA Leiden, The Netherlands. Tel.: 31-071-5274213; Fax: 31-071-5274357; E-mail: abrahams@fwncism1.leidenuniv.nl.

[1] The abbreviations used are: CAV, chicken anemia virus; CV, column volume; DAPI, 2,4-diamidino-2-phenylindole; DLS, dynamic light scattering; IPTG, isopropyl-β-D-1-thiogalactoside; mAb, monoclonal antibody; MBP, maltose-binding protein; MM, molecular mass; NES, nuclear export signal; NTA, nitrilotriacetic acid; OG, *N*-octylthioglucoside; ORF, open reading frame; R_H, hydrodynamic radius; PBS, phosphate-buffered saline; CHAPSO, 3-[(3-cholamidopropyl)dimethylammonio]-2-hydroxy-1-propanesulfonic acid.

[2] A. Danen-van Oorschot, Y.-H. Zhang, S. R. Leliveld, J. L. Rohn, M. C. M. J. Seelen, M. W. Bolk, A. van Zon, S. J. Erkeland, J. P. Abrahams, D. Mumberg, and M. H. M. Noteborn, manuscript in preparation.

[3] Y.-H. Zhang, S. R. Leliveld, K. Kooistra, C. Molenaar, J. Rohn, H. J. Tanke, J. P. Abrahams, and M. H. M. Noteborn, submitted manuscript.

TABLE I
Apoptin expression constructs

Construct	Sequence	Bacterial/Mammalian	MW[1]/pI[1]
MBP	MBP-$(N)_{10}$-LVPRGSGG	bacterial	42.6/5.1
MBP-Apoptin	MBP-$(N)_{10}$-LVPRGSGG-Apoptin(1–121)	bacterial/mammalian	55.8/6.5
MBP-Apoptin(1–69)-H_6	MBP-$(N)_{10}$-LVPRGSGG-Apoptin(1–69)-LE-$(H)_6$	bacterial	50.8/5.6
MBP-Apoptin(66–121)	MBP-$(N)_{10}$-LVPRGSGG-Apoptin(66–121)	bacterial	49.1/6.1
MBP-Apoptin(80–121)	MBP-$(N)_{10}$-LVPRGSGG-Apoptin(80–121)	mammalian	47.4/6.4
Apoptin-H_6	Apoptin(1–121)-$(A)_3$-LE-$(H)_6$	bacterial	14.5/9.8
Apoptin(1–69)-H_6	Apoptin(1–69)-LE-$(H)_6$	bacterial	8.3/6.6

69)H_6, including the downstream T7 terminator of pET-22b, and cloned into pMalTB at *Bam*HI and *Sal*I.

pMalTBVp3dN66, MBP Fusion of C-terminal 56 Residues of Apoptin (MBP-Apoptin(66–121))—The truncated Apoptin(66–121) ORF, including the stop codon, was cloned in pMalTB at *Bam*HI and *Sal*I.

pcDNA3.1mychis(−)-MVp3—The full MBP-Apoptin ORF, including the stop codon, was amplified by PCR from pMalTBVp3 and cloned at *Nhe*I and *Kpn*I in pcDNA3.1*mychis*(−) type B (Invitrogen). Expression is controlled by a constitutive cytomegalovirus promoter.

pcDNA3.1mychis(−)-MVp3(80–121)—pcDNA3.1mychis(−)-MVp3 was digested with *Bam*HI and *Kpn*I, removing the full Apoptin ORF. Subsequently, the truncated Apoptin(80–121) ORF was amplified by PCR and cloned into the linearized vector at *Bam*HI and *Kpn*I.

All clones were confirmed by automated fluorescent sequencing. Table I summarizes the protein constructs we generated.

Bacterial Expression of Apoptin Constructs

Medium to large scale expression was performed in either of two set-ups as follows: 1) 500 ml of expression medium in a 2-liter three-baffled flask (Bellco Glass Inc.) (250 rpm, 37 °C); or 2) a 1.8-liter bench-top fermentor (Biospec Products Inc.) (maximum agitation and aeration, 37 °C). In both cases, a few drops of anti-foam A (Sigma) were added directly prior to inoculation. For expression of MBP fusion proteins, the LB medium was supplemented with 0.2% glucose to suppress the expression of endogenous *E. coli* α-amylases, which might interfere with affinity purification of the fusion protein. *E. coli* BL21(λDE3) $CaCl_2$-competent cells were transformed with one of the Apoptin constructs described above. A single transformant colony was grown overnight in LB (+0.2% glucose), supplemented with 200 μg/ml carbenicillin (Duchefa) and if necessary with 0.1 mM $ZnSO_4$. After resuspending the cells in fresh medium, a volume of expression culture (LB + 0.2% glucose, +100 μg/ml carbenicillin, ±0.1 mM $ZnSO_4$) was inoculated 1 in 50. Upon reaching an A_{600} of ~0.8 (2 to 3 h), expression was induced by adding 1 mM IPTG. After 3 to 4 h (final A_{600} = 3 to 5), the cells were harvested and lysed using a BeadBeater (Biospec Products Inc.). Lysis buffers were as follows: 1) for MBP, MBP-Apoptin, MBP-Apoptin(1–69)-H_6, and MBP-Apoptin(66–121): 25 mM HEPES, pH 7.4, 500 mM NaCl, 10% glycerol, 5 mM reduced glutathione (GSH) (Sigma), 2 mM $MgCl_2$, 1× protease inhibitor mixture (EDTA-free) (Roche Molecular Biochemicals), DNase I (10 to 50 μg/ml) (Roche Molecular Biochemicals); 2) for Apoptin-H_6: 1× PBS, 2 mM $MgCl_2$, 1 mM phenylmethylsulfonyl fluoride (Invitrogen), DNase I; 3) Apoptin(1–69)H_6, 50 mM KPO_4, pH 7.4, 2.5 mM imidazole (Fluka), 300 mM NaCl, 2 mM $MgCl_2$, DNase I, protease inhibitor mixture, 2.5 mM GSH. The glass bead/lysate slurry was filtered (Whatmann 3MM) and centrifuged at 29,000 × *g* for 15 min. Finally, lysates were fully cleared by filtering over a 0.22-μm filter.

Purification of E. coli-expressed Protein

MBP-Apoptin and MBP-Apoptin(66–121)—The cleared lysate of a 1-liter expression culture was passed twice over an amylose column (2.5 × 20 cm), equilibrated in 20 mM HEPES, pH 7.4, 500 mM NaCl, 10% glycerol, 1 mM EDTA, or 0.1 mM $ZnSO_4$, under gravity flow at 4 °C. The column was washed with 5 column volumes (CV) of 20 mM HEPES, pH 7.4, 1 M NaCl, 1 mM EDTA, or 0.1 mM $ZnSO_4$ followed by 5 CVs of 20 mM HEPES, pH 7.4, 50 mM NaCl, 1 mM EDTA, or 0.1 mM $ZnSO_4$. The column was then eluted with 20 mM HEPES, pH 7.4, 50 mM NaCl, 1 mM EDTA, or 0.1 mM $ZnSO_4$, 10 mM maltose (Fluka). For all MBP fusion proteins, phenylmethylsulfonyl fluoride (0.5 mM) was directly added to the eluate to prevent degradation by traces of *E. coli* proteases. After filtering, the eluate was loaded on an analytical cation exchange column (UNO-S12) (Bio-Rad), equilibrated at 3 ml/min in 20 mM HEPES, pH 7.4, 50 mM NaCl, 1 mM EDTA, or 0.1 mM $ZnSO_4$. After extensive washing, the column was eluted with a 200-ml linear gradient (50–1000 mM NaCl, 5-ml fractions). Appropriate fractions were pooled and dialyzed against PBS (CelluSep T1 membranes, molecular mass cut-off 3.5 kDa; Membrane Filtration Products Inc.). MBP-Apoptin and MBP-Apoptin(66–121) were concentrated on a Biomax 5K or 10K Ultrafree spin filter (Millipore) to 40 and 10 mg/ml, respectively. As a rule, solutions of MBP-Apoptin fusion proteins were never subjected to freeze/thawing and stored at 4 °C for up to one month. We noticed that MBP-Apoptin, but not MBP alone, formed insoluble aggregates when incubated at ~1 mg/ml in PBS, 1 mM EDTA, 1% (32 mM) *N*-octylthioglucoside (OG) (Roche Molecular Biochemicals) for 1 h at 30 °C (data not shown). Only a small amount of MBP-Apoptin remained in solution under these conditions, as tested by Bradford protein assay (Bio-Rad). We did not observe such an effect when OG was replaced by CHAPSO (0.5%; Sigma) or Triton X-100 (1%; Roche Molecular Biochemicals).

Apoptin-H_6—Starting with a 1.8-liter expression, the pellet after lysis was resuspended in PBS, 0.5% Triton X-100 (Roche Molecular Biochemicals) and stirred at room temperature for 1 h. The suspension was then centrifuged at 29,000 × *g* for 20 min, after which the inclusion bodies were washed once with PBS. They were then resuspended in 50 mM HEPES, pH 7.4, 20 mM glycine, 2 mM EDTA, 20 mM DL-dithiothreitol, 8 M urea (molecular biology grade) (Invitrogen) and stirred overnight at 4 °C. The cleared supernatant was then loaded on a UNO-S12 column, equilibrated at 3 ml/min in 20 mM KPO_4, pH 7.4, 2.5 mM imidazole, 2 mM GSH, 6 M urea. After washing, the column was eluted with a 160-ml linear gradient (0–1 M NaCl, 5-ml fractions). Appropriate fractions were pooled and stored at −80 °C if not used immediately afterward. UNO-S12-cleaned Apoptin-H_6 was mixed with a suspension of 10 to 15 ml of Ni^{2+}-nitrilotriacetic acid (NTA)-agarose (Qiagen), equilibrated in 20 mM KPO_4, pH 7.4, 2.5 mM imidazole, 500 mM NaCl, 2 mM GSH, 6 M urea, and stirred at 4 °C for 2 h. The resin was packed into a column, which was subsequently washed with 5 CVs of 20 mM KPO_4, pH 7.4, 20 mM imidazole, 500 mM NaCl, 2 mM GSH, 6 M guanidinium hydrochloride (Invitrogen). The denaturant was then removed, in one step, by washing with 5 CVs of 20 mM KPO_4, pH 6.5, 5 mM imidazole, 400 mM NaCl, 2 mM GSH, 2 mM $MgCl_2$. The protein was eluted with the same buffer, supplemented with 500 mM imidazole. All Ni^{2+} traces were removed completely by adding 5 mM EDTA to the eluted protein and dialyzing it against 20 mM KPO_4, pH 6.5, 400 mM NaCl, 2 mM $MgCl_2$. Refolded Apoptin-H_6 was concentrated on a Centricon YM3 filter (Amicon) to 10 mg/ml. Solutions of refolded Apoptin-H_6 were never subjected to freeze/thawing and were stored for up to one month at 4 °C.

MBP-Apoptin(1–69)-H_6—The cleared lysate of a 1-liter expression was applied to an amylose column, as described above. After washing, the fusion protein was eluted in 50 mM KPO_4, pH 7.4, 2.5 mM imidazole, 300 mM NaCl, 10 mM maltose. The eluate was filtered and loaded on a Ni^{2+}-NTA-agarose column (1.5 × 5 cm), which was washed with 50 mM KPO_4, pH 7.4, 30 mM imidazole, 300 mM NaCl. The protein was eluted with 50 mM KPO_4, pH 7.4, 300 mM imidazole, 300 mM NaCl and dialyzed against PBS, 0.5 mM EDTA.

MBP—Non-fused MBP was purified from IPTG-induced *E. coli* BL21(λDE3) transformed with pMalTB. After binding to amylose, the column was washed with 20 mM Tris-HCl, pH 7.4, 1 mM EDTA. MBP was then eluted with 20 mM Tris-HCl, pH 7.4, 1 mM EDTA, 10 mM maltose and loaded on an analytical anion exchange column (UNO-Q1; Bio-Rad). The column was eluted with a 20-ml linear gradient (0–1 M NaCl, 1-ml fractions). MBP-containing fractions (1 to 5 mg/ml) were dialyzed against PBS and then flash-frozen in liquid nitrogen and stored at −20 °C.

Apoptin(1–69)-H_6—The cleared lysate of a 1-liter culture was loaded on a 5-ml Ni^{2+}-NTA-agarose (1.5 × 3 cm) column. The column was washed with lysis buffer, supplemented with 100 mM imidazole, and then eluted with 20 mM KPO_4, pH 7.4, 500 mM imidazole, 500 mM NaCl. After adding EDTA, the eluate was dialyzed to 20 mM KPO_4, pH 6.5, 400 mM NaCl, 2 mM $MgCl_2$. Apoptin(1–69)-H_6 was concentrated on a Centricon YM3 filter (Amicon) to 10 mg/ml.

Protein Concentration Determination

All protein concentrations were determined from A_{280}. The extinction coefficient of MBP-Apoptin and Apoptin-H_6 at 280 nm (mg/ml/cm) was 1.0 ± 0.1 and 0.10 ± 0.01, respectively. The molecular mass of MBP-Apoptin and Apoptin-H_6 was taken as 55.8 and 14.5 kDa per monomer, respectively.

Size Exclusion Chromatography

Samples were run as follows: 1) Sephacryl S100 HR (1.0 × 48 cm; Amersham Biosciences), which was calibrated with blue dextran (>2 MDa; Sigma) and Ponceau S (0.76 kDa; Sigma) at a flow rate of 11.5 cm/h in a sample load of 500 μl; or 2) Superose 6 HR 10/30 (Amersham Biosciences), which was calibrated with a size exclusion chromatography calibration kit (Bio-Rad) (670, 158, 44, 17, and 1.35 kDa) at a flow rate of 0.2 to 0.4 ml/min in a sample load of 100 μl. For the second set of conditions (Superose 6 HR), linear regression analysis of the elution profile of the calibration run yielded log[molecular mass (kDa)] = 7.773 − (0.365)[ml eluens].

Dynamic Light Scattering

All dynamic light scattering measurements were recorded on a DynaPro-MS/X (Protein Solutions Inc.) at room temperature. Bovine serum albumin was used as a control (0.5 mg/ml in PBS, 0.5 mM EDTA). MBP-Apoptin was measured at 10 μM (monomer concentration) in PBS, 0.5 mM EDTA, and refolded Apoptin-H_6 at 35 μM (monomers) in 20 mM KPO_4, pH 6.5, 400 mM NaCl, 2 mM $MgCl_2$. Per experiment, between 20 and 40 measurements (10-s intervals) were collected. The hydrodynamic radius of the particle (R_H) was determined by averaging the results of at least three separate experiments. Protein molecular mass was estimated from the R_H by the equation, MM (kDa) = $[1.68 \times R_H]^{2.34}$.

Circular Dichroism Spectroscopy

Far-UV circular dichroism spectra were recorded on a Jasco J-715 spectrometer. Spectrometer settings were as follows: wavelength range, 190–260 nm; cell width, 1 mm; scan speed, 50 nm/min; response time, 1.0 s; bandwidth, 1.0 nm; pitch, 0.1 nm. Spectra were averaged over eight acquisitions. Throughout the measurements, the spectrometer was flushed with O_2-free N_2 at 10 liters/min. Cell temperature was maintained at 20 °C by a Jasco PTC-348WI Peltier element. MBP-Apoptin was dialyzed to 10 mM KPO_4, pH 6.5, 0.1 mM EDTA, or 0.1 mM $ZnSO_4$, and refolded Apoptin-H_6 was dialyzed to 20 mM KPO_4, pH 6.5, 1 mM $MgSO_4$, or 0.1 mM $ZnSO_4$. All samples and buffers were filtered and degassed directly prior to measurement.

Fluorescence Measurements

Fluorescence emission and excitation spectra were recorded on a PerkinElmer Life Sciences LS-50B. Fluorimeter settings were as follows: slit width, 6 nm; scan speed, 120 nm/min; excitation wavelength, 280 nm. Final spectra were obtained by averaging three separate spectra. Background emission and excitation spectra were recorded of the respective filtered buffers. The concentration of refolded Apoptin-H_6 was 55 μM (monomer concentration) in refolding buffer (20 mM KPO_4, pH 6.5, 400 mM NaCl, 2 mM $MgCl_2$). The concentration of free tyrosine (L-Tyr) was 7.5 μM in Apoptin-H_6 dialysis buffer, pH 6.5, and 500 μM in 50 mM Na_3PO_4, pH 12, 1 mM EDTA.

Scanning Force and Electron Microscopic Analysis

Biotin Labeling—Fresh MBP-Apoptin (20 mg/ml, 0.1 M $NaHCO_3$, pH 8.3) was incubated with 5 mM sulfo-NHS-LC-biotin (Molecular Probes, Inc.) at room temperature for 3 h. The reaction was terminated by adding 10 mM ethanolamine. To remove unincorporated label, the labeled protein was passed over a PD-10 desalting column (Amersham Biosciences), equilibrated in 20 mM HEPES, pH 7.4, 0.1 mM EDTA.

Electron Microscopy—Both labeled and unlabeled MBP-Apoptin (30 mg/ml, in 20 mM HEPES, pH 7.4, 0.1 mM EDTA) were filtered over 0.22-μm spinfilters (Ultrafree-MC; Millipore) and adsorbed to a carbon-coated polioform layer grid. Both samples were incubated with concentrated streptavidin-gold conjugate (gold particle diameter, 5 nm) (Kirkegaard & Perry Laboratories Inc.) and stained with 3% uranyl acetate. Electron microscopy was performed on a Philips TEM 410 transmission electron microscope.

Scanning Force Microscopy—90 ng of purified MBP-Apoptin (in 10 μl of 5 mM HEPES, pH 7.9, 3 mM KCl, 5.5 mM $MgCl_2$) was incubated at 37 °C for 15 min and then deposited on a disc of freshly cleaved mica (Ted Pella Inc.). After 20 s, the mica was gently rinsed with high pressure liquid chromatography water. Excess water was removed, and the disc was dried with a steady flow of 0.22 μm of filtered air. Images were acquired on a Nanoscope IIIa (Digital Instruments Inc.), operating in tapping mode in air with a type E scanner. Silicon tips were obtained from Digital Instruments.

SDS-PAGE and Western Blotting

SDS-PAGE—Protein samples were run on 7.5–15% SDS-PAGE gels, either under reducing or non-reducing conditions, *i.e.* with or without β-mercaptoethanol in the sample buffer. 1× SDS-PAGE sample buffer contained 20 mM Tris-HCl, pH 6.8, 0.01% bromphenol blue, 1% SDS, 10% glycerol, 1% β-mercaptoethanol. Gels were stained with Coomassie Brilliant Blue (Bio-Rad).

Western Blotting and Dot Blotting—Samples were run on SDS-PAGE and blotted onto Immunoblot polyvinylidene difluoride membranes (Bio-Rad) or dot blotted directly onto polyvinylidene difluoride after denaturation in 1× SDS-PAGE sample buffer (95 °C for 5 min). Blots were probed with the anti-Apoptin monoclonal antibody 111.3 (epitope, residues 18 to 23) (2) or with the polyclonal anti-Apoptin antibody αVP3-C, which has an epitope range comprising residues 79 to 90 (9). Blots were subsequently incubated with an appropriate horseradish peroxidase-conjugated secondary antibody and developed by enhanced chemiluminescence.

Fluorescent Zinc Assay

Calibration Curve—A concentration range of $ZnSO_4$ (1 to 20 μM) (Fluka) was prepared in assay buffer (50 mM HEPES, pH 7.4, 0.2% SDS), to which 200 nM FluoZin-1 (Molecular Probes) was added to from a 2 mM stock solution in water. Fluorescence spectra were recorded after 15 min of equilibration at room temperature. Spectra were adjusted for background fluorescence, which was determined from a sample of FluoZin-1, to which 5 mM EDTA had been added. Fluorimeter settings were as follows: slit width, 4 nm; scan speed, 120 nm/min; excitation wavelength, 495 nm.

Sample Preparation—Protein samples were as follows. 1) MBP-Apoptin was expressed in the presence of 0.1 mM $ZnSO_4$ and purified without using EDTA. 2) MBP-Apoptin, expressed without additional Zn^{2+} and treated with EDTA, was incubated with a 10-fold molar excess of $ZnSO_4$ overnight at 4 °C (in PBS). Both samples were desalted on a PD-10 column, equilibrated in 50 mM HEPES, pH 7.4, and then denatured in 0.5% SDS (95 °C for 5 min). After cooling to room temperature, the samples were diluted in assay buffer to 10 μM final protein concentration (monomers) and 0.2% final SDS concentration. Fluorescence spectra were recorded after addition of FluoZin-1.

Fluorescent Labeling and Chemical Cross-linking

Fluorescent Labeling—The number of solvent-exposed Cys residues per MBP-Apoptin monomer was determined using 5,5′-dithiobis(2-nitrobenzoic acid) (Sigma) (10). Fresh MBP-Apoptin (5 mg/ml, PBS) was incubated with 2 mM of fluorescein-5-maleimide (Molecular Probes), diluted from a freshly prepared 20 mM stock solution in 50 mM Na_3PO_4, pH 12, and incubated overnight at 4 °C in the dark. The labeling reaction was stopped by adding 10 mM β-mercaptoethanol, after which unincorporated label was removed by passing the protein over a PD-10 column (Amersham Biosciences), equilibrated in PBS. The level of label incorporation was determined from the equation, $[A/EC] \times [MM/C]$, where A is the absorbance of the label, C is the concentration of labeled protein (in mg/ml), EC is the molar extinction coefficient of the label (cm/M), and MM is the molecular mass of the protein (in Da).

Cross-linking—Following labeling with fluorescein-5-maleimide, the protein (3 mg/ml) was incubated with 0.05% glutaraldehyde, diluted from a 8% stock solution in water (grade I; Sigma), for 3 min at 30 °C (in the dark). The reaction was stopped by adding 50 mM β-alanine (Fluka). After 20 min, the protein was passed over a PD-10 column, equilibrated in PBS.

Incubation of Recombinant MBP-Apoptin in Saos-2 and VH10 Lysates in Low Detergent Buffer

Saos-2 cells, which are human tumor cells derived from osteosarcoma, and VH10 cells, which are normal human fibroblasts, were grown to around 50% confluency. The cells were washed with cold PBS and harvested in ice-cold 25 mM HEPES, pH 7.4, 150 mM KCl, 2 mM $MgCl_2$, 5 mM dithiothreitol, 2.5 mM benzamidine hydrochloride (Sigma), 0.25% CHAPSO (Sigma). The suspensions were sonicated on ice, after which insoluble material was removed by centrifugation at 29,000 × *g* for 20 min. After determining the respective protein concentrations, MBP-Apoptin was added to 5% (w/w), which was estimated to be the average ratio of MBP-Apoptin to cytoplasmic protein in microinjected cells (7, 8).

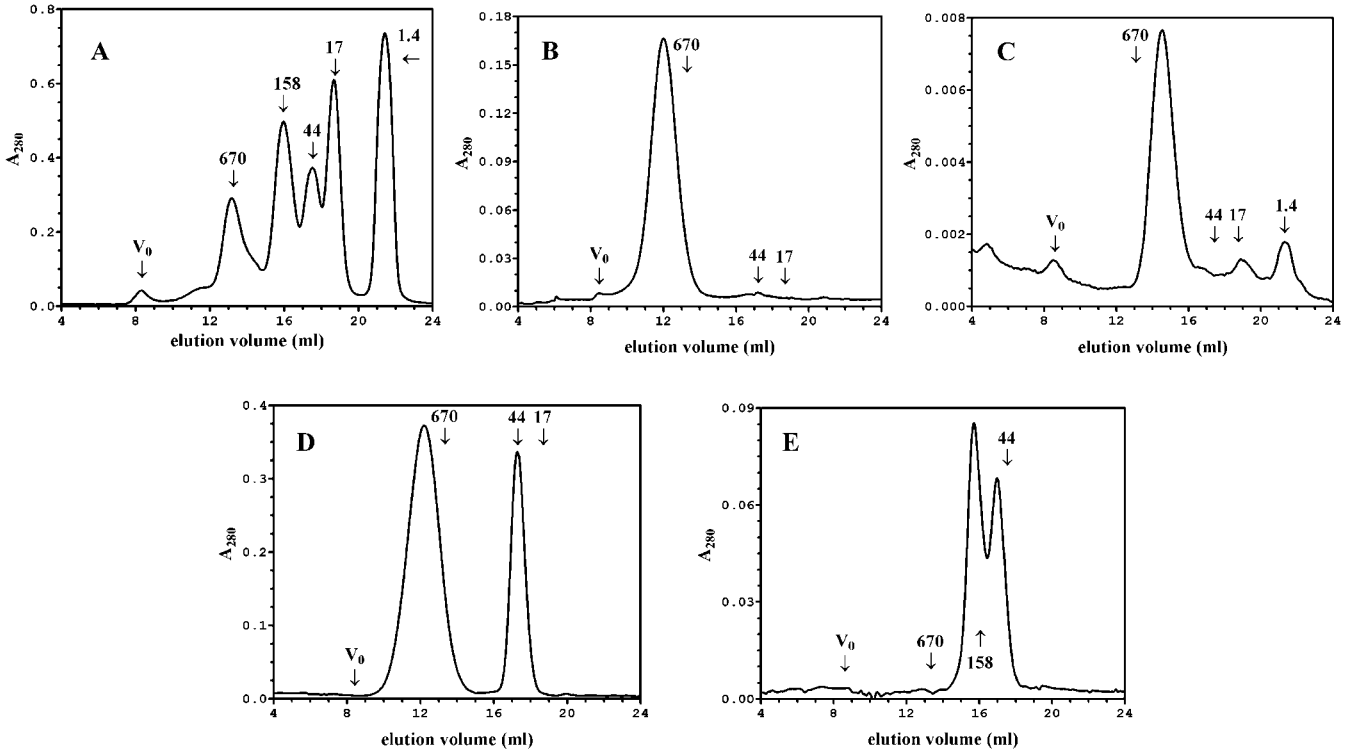

FIG. 1. **Recombinant MBP-Apoptin and Apoptin-H_6 form non-covalent multimeric complexes.** Size exclusion chromatography of MBP-Apoptin and refolded Apoptin-H_6 on Superose 6 HR 10/30 are shown. *A*, calibration with gel filtration standards in PBS indicating the resolving power of the column was as follows: thyroglobulin, 670 kDa; γ-globulin, 158 kDa; ovalbumin, 44 kDa; myoglobin, 17 kDa; vitamin B12, 1.4 kDa. *B*, MBP-Apoptin, 10 mg/ml in 2× PBS, 0.5% CHAPSO. The low intensity peak at about 17 ml elution volume was caused by a trace amount of non-fused MBP. *C*, refolded Apoptin-H_6, 7 mg/ml in 20 mM KPO_4, pH 6.5, 400 mM NaCl, 2 mM $MgCl_2$, 5 mM Cys-HCl. *D*, purified MBP-Apoptin(1–69)-H_6, 15 mg/ml, in PBS. During purification, proteolytic cleavage occurred at the thrombin cleavage sites in the peptide linker between MBP and Apoptin(1–69)-H_6. The peak at 12.5 ml elution volume is the intact fusion protein, the peak at 17.5 ml is MBP alone. *E*, purified MBP-Apoptin(66–121), 5 mg/ml in PBS.

Samples were incubated for 30 min at 30 °C, in the presence of 1 mM ATP and 20 mM $MgCl_2$, and for 2 and 24 h at 4 °C, without additives. Following incubation, samples were fractionated on Superose 6 HR 10/30. Prior to fractionation, any precipitated material was pelleted by centrifugation at 29,000 × *g* for 20 min, after which the pellets were washed with lysis buffer. All pellets and fractions were dot blotted, using 10 μl per sample, as described above. Dot blots were probed with mAb 111.3.

Microinjection

Saos-2 and VH10 cells were cultured in Dulbecco's modified Eagle's medium containing 10% fetal calf serum, penicillin and streptomycin (Invitrogen). Cells were seeded in 35-mm tissue glass-bottomed culture dishes and grown to 30 to 40% confluency prior to microinjection. During microinjection, cells were incubated in RPMI 1640 medium (25 mM HEPES, pH 7.2, 5% fetal calf serum, penicillin, and streptomycin) at 37 °C. Cells were returned to Dulbecco's modified Eagle's medium directly after microinjection. Microinjection was performed with 0.5-μm microneedles (sterile femtotips II; Eppendorf) under an inverted microscope (Axiovert 135 TV; Zeiss), equipped with a programmable microinjector (IM 300; Narishige Co.) and a joystick hydraulic micromanipulator (MMO-202; Narishige Co.). Fluorescein-labeled, cross-linked MBP-Apoptin (3 mg/ml, in PBS) was combined with lysine-fixable rhodamine-dextran (Molecular Probes) to mark injected cells. Directly prior to injection, protein samples were filtered over 0.22 μm or centrifuged at 15,000 × *g* for 15 min. An injection pressure of 0.5 to 1.0 pounds/square inch, and an injection time of 0.2 to 0.5 s was used. For analysis of apoptotic activity, 100 cells were injected per dish.

Transient Transfection and Protein Extraction

Saos-2 cells were seeded in 9-cm plates at 20% confluency and transfected with 7 μg of DNA using FuGENE 6.0 (Roche Molecular Biochemicals) according to the manufacturer's protocol, pcDNA3.1mychis(−)-MVp3, pcDNA3.1mychis(−)-MVp3 (80–121) (3:1 μl/μg FuGENE:DNA ratio), or mock-transfected. For analysis of protein solubility, cells were trypsinized and washed with 1× PBS 2 days after transfection. Cells were pooled from two dishes per construct and resuspended in 200 μl of 20 mM Tris-HCl, pH 7.5, 250 mM NaCl, 5 mM EDTA, 0.1% Triton X-100, 20 mM β-glycerophosphate, 5 mM NaF, 5 mM GSH, 2× protease inhibitor mixture (Roche Molecular Biochemicals), and left on ice for 30 min. Cell debris and the bulk of the insoluble protein fraction were pelleted by centrifugation at 10,000 × *g* for 20 min at 4 °C. After separating supernatant (S10) and pellet (P10), we centrifuged the supernatant at 30,000 × *g* for 20 min, yielding S30 and P30. Protein samples were Western blotted, as described above, and blots were stained with αVP3-C.

(Immuno)fluorescence Microscopy

Microinjection—2 and 24 h after injection, cells were fixed sequentially with PBS, 1% freshly prepared formaldehyde (10 min) and then 100% cold MeOH (5 min) and 80% cold acetone (2 min). Fluorescein-labeled, cross-linked MBP-Apoptin was detected by direct fluorescence. The apoptotic condition of individual cells was deduced from their nuclear morphology after staining with 2,4-diamidino-2-phenylindole (DAPI).

Transient Transfection—In a parallel experiment, Saos-2 cells were grown on coverslips in 9-cm plates and transfected as described above, fixed using fresh 1:1 methanol:acetone for 5 min, and stained with a mouse monoclonal antibody that recognized MBP (clone R29.6; Abcam). An appropriate fluorescein isothiocyanate-labeled secondary antibody was added, and the cells were mounted in DAPI/DABCO(1,4-diazabicyclo[2.2.2]octane)/glycerol. Again, apoptotic cells were scored on the basis of their nuclear morphology. Detection of MBP-Apoptin with αVP3-C produced comparable results.

RESULTS

Recombinant Apoptin Forms Non-covalent Multimeric Complexes

MBP-Apoptin—In *E. coli*, soluble MBP-Apoptin was expressed with a yield of up to 100 mg per liter of culture. After affinity chromatography on amylose resin and cation exchange chromatography, MBP-Apoptin migrated as a stable multim-

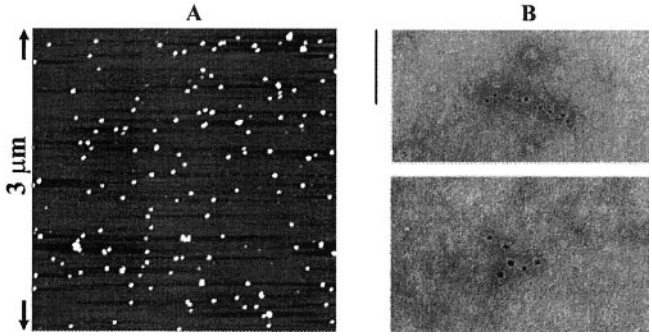

FIG. 2. **Analysis of MBP-Apoptin multimers by scanning force microscopy and electron microscopy.** The Apoptin multimeric complex is globular and has a diameter of about 40 nm. *A*, scanning force microscopy analysis was as follows: MBP-Apoptin (in 5 mM HEPES, pH 7.9, 5.5 mM $MgCl_2$, 3 mM KCl) was deposited onto freshly cleaved mica and then air-dried. The surface area is 3 × 3 μm. Height is indicated in *grayscale*, and the *bar* is from 0.0 (*black*) to 1.5 nm (*gray*). *B*, electron microscopy analysis was as follows: biotin-labeled MBP-Apoptin (30 mg/ml) was adsorbed onto a carbon-coated polioform layer grid and incubated with a streptavidin-gold conjugate (diameter gold particles = 5 nm). Between 5 and 10% of globules showed gold binding, whereas a-selective binding was less than 0.1%. Negative staining was done with 3% uranyl acetate. *Bar* represents 100 nm.

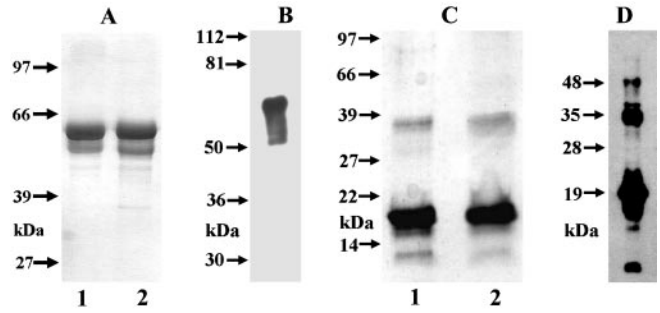

FIG. 3. **Apoptin degradation products co-purify with full-length recombinant protein in the multimeric complex.** SDS-PAGE and Western blot analysis of purified MBP-Apoptin and refolded Apoptin-H_6 are shown. MBP-Apoptin was run on 10% SDS-PAGE, and refolded Apoptin-H_6 was run on 13.5% SDS-PAGE. Western blots were probed with the anti-Apoptin monoclonal antibody mAb 111.3. *A*, purified MBP-Apoptin. *1*, non-reduced; *2*, reduced. *B*, Western blot of MBP-Apoptin. *C*, purified, refolded Apoptin-H_6. *1*, reduced; *2*, non-reduced. *D*, Western blot of refolded Apoptin-H_6.

eric complex, with a molecular mass of 2.5 ± 0.3 MDa, on an analytical size exclusion chromatography column (Superose 6 HR 10/30) (Fig. 1, *A* and *B*). The molecular mass of the MBP-Apoptin monomer is 56 kDa; see Table I. Analysis of purified MBP-Apoptin by scanning force microscopy and electron microscopy showed a uniform population of globular particles with a radius of ~40 nm (Fig. 2, *A* and *B*). Dynamic light scattering (DLS[1]) confirmed that the MBP-Apoptin complex is present as a single solute species with an average R_H of 17.9 ± 2.0 nm, which corresponds to a diameter of 36 ± 4.0 nm and an estimated molecular mass of 2.9 ± 0.6 MDa. The variation in the average R_H of the MBP-Apoptin particle among four separate protein batches remained within experimental error (16 to 20 nm). The multimerization of MBP-Apoptin was independent of the protein concentration (0.5 to 25 mg/ml), ionic strength (up to 0.4 M NaCl), and the presence of detergent (0.5% CHAPSO or 1% Triton X-100). Despite the high stability of the complex, there were no covalent bonds between individual MBP-Apoptin monomers, because only monomers could be observed upon boiling in SDS followed by SDS-PAGE under non-reducing conditions (Fig. 3*A*). We noticed that MBP-Apoptin precipitated nearly completely when incubated in 1% OG (in PBS), a non-denaturing detergent, for 1 h at 30 °C (data not shown). Because MBP alone did not precipitate under the same conditions, it appeared that *N*-octylthioglucoside selectively destabilized the Apoptin multimer. This result suggests that hydrophobic interactions play an essential role in the formation of Apoptin protein multimers.

In addition to the full-length MBP-Apoptin fusion protein, which migrated as a 58.5-kDa species on SDS-PAGE, three less-abundant expression products of 56.7, 53.3, and 50.1 kDa consistently co-purified with the MBP-Apoptin multimer. All three could be detected with the anti-Apoptin mAb 111.3 (Fig. 3*B*). These products could not be removed under native conditions, demonstrating that the degradation products were still incorporated into the MBP-Apoptin complex. The linker peptide that connects the MBP and Apoptin moieties contains a thrombin cleavage site. When the fusion protein was digested with thrombin, cleaved-off MBP was released from the complex, whereas the Apoptin moieties remained part of it, indicating that the multimerization behavior of MBP-Apoptin depended entirely on the Apoptin moiety (data not shown).

Apoptin-H_6—In *E. coli*, inclusion bodies of Apoptin-H_6 were expressed with a yield of up to 40 mg per liter of culture. Manipulating growth or lysis conditions did not increase the solubility of Apoptin-H_6. After solubilization in 8 M urea, Apoptin-H_6 was purified to ~90% homogeneity by cation exchange chromatography under denaturing conditions (6 M urea). It could be refolded with a net efficiency of ~50% in a single step while bound to Ni^{2+}-NTA-agarose. On Superose 6 HR 10/30, refolded Apoptin-H_6 migrated as a single species with a molecular mass of 400 ± 50 kDa, independent of protein concentration (1 to 7 mg/ml) (Fig. 1*C*). The molecular mass of the Apoptin-H_6 monomer is 14.5 kDa; see Table I. The two additional peaks of 30 and 10 kDa in the Superose 6 elution profile were unlikely to contain Apoptin as they were not recognized by the Apoptin-specific antibody mAb 111.3. DLS confirmed the particle size, indicating a single solute species with an R_H of 8.5 ± 1.0 nm, corresponding to a molecular mass of 500 ± 100 kDa. The variation in complex size among three separate protein batches remained within experimental error (8 to 10 nm).

Like the MBP-Apoptin complex, the Apoptin-H_6 complex was non-covalent, as shown by non-reducing SDS-PAGE (Fig. 3*C*). A number of additional species migrating with apparent molecular masses of 8, 34, and 48 kDa could be detected by mAb 111.3 (Fig. 3*D*). The smallest mAb 111.3-reactive species (8 kDa) corresponded to an N-terminal fragment lacking the C-terminal hexahistidine tag. As in the MBP-Apoptin complexes, fragments truncated at the C terminus remained associated and co-purified.

Mapping the Regions Required for Multimerization: N- and C-terminal Domains of Apoptin—To evaluate the ability of fragments of Apoptin to form multimers, Apoptin's N-terminal 69 residues and C-terminal 56 residues (66–121) were cloned separately as MBP fusion proteins. The MBP-Apoptin(1–69) fusion also contained a C-terminal hexahistidine tag to facilitate further purification. In *E. coli*, soluble MBP-Apoptin(1–69)-H_6 was expressed with yields of up to 100 mg per liter of culture. It displayed the same elution profile on size exclusion chromatography as did full-length MBP-Apoptin(1–121), indicating that the complex is about 2.5 MDa in size (Fig. 1*D*). As with the full-length MBP-Apoptin complex, Apoptin(1–69)-H_6 with its MBP moiety cleaved off co-eluted with the intact fusion protein (data not shown).

In *E. coli*, soluble Apoptin(1–69)-H_6 was expressed with a yield of up to 2 mg per liter of culture. After Ni^{2+}-NTA-agarose purification, the homogeneity of Apoptin(1–69)-H_6 was ~80%. When the Ni^{2+}-NTA-agarose eluate was fractionated on a Sephacryl S100 HR gel filtration column, the Apoptin(1–69)-H_6 could only be recovered from the void volume. This

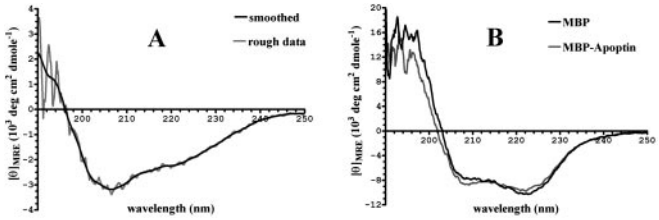

FIG. 4. **Circular dichroism spectra of MBP-Apoptin and refolded Apoptin-H_6.** Apoptin has a low secondary structure content but may contain regions with β-sheet or β-turn structure. *A*, CD spectrum of refolded Apoptin-H_6, 40 μM in 20 mM KPO_4, pH 6.5, 1 mM $MgSO_4$. *B*, CD spectrum of MBP-Apoptin and MBP, both 6 μM (monomer) in 10 mM KPO_4, pH 6.5, 0.1 mM EDTA.

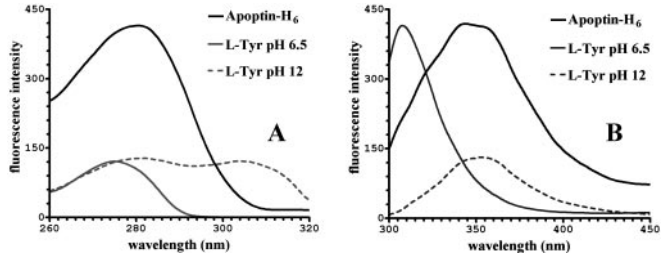

FIG. 5. **Intrinsic fluorescence emission and excitation spectrum of refolded Apoptin-H_6.** The single Tyr residue of Apoptin (Tyr^{95}) is involved in a stable hydrogen-bonding network. *A*, excitation spectrum; *B*, emission spectrum.

finding indicated that Apoptin(1–69)-H_6 formed a complex of at least 100 kDa in size under non-denaturing conditions (data not shown). The molecular mass of the Apoptin(1–69)-H_6 is 8.3 kDa; see Table I.

MBP-Apoptin(66–121) was expressed in soluble form to ~50 mg per liter of culture. Purified MBP-Apoptin(66–121) migrated at ~50 kDa on SDS-PAGE. In contrast to the full-length fusion protein, MBP-Apoptin(66–121) consisted exclusively of two species of ~200 and 60 kDa, which may correspond to an equilibrium between a monomer and a di- or trimer (Fig. 1*E*). The molecular mass of MBP-Apoptin(66–121) is 49 kDa; see Table I. DLS analysis indicated that there was only one solute species present, with an R_H of 4.6 ± 0.8 nm, which corresponds to an average molecular mass of 120 ± 50 kDa. Regardless of the precise nature of the two species, this result shows that the C-terminal domain of Apoptin on its own is unable to form the type of higher order multimers such as MBP-Apoptin(1–121) does. Taken together, these results demonstrate that the N-terminal 69 residues of Apoptin contain sufficient structural elements to account for its multimerization behavior.

Apoptin Has Little if Any Ordered Structure

Next, we examined whether recombinant Apoptin protein harbors any secondary or tertiary structure, using circular dichroism (CD) and fluorescence spectroscopy.

CD Spectroscopy—The far-UV CD spectrum of refolded Apoptin-H_6 (Fig. 4*A*) showed a very small mean residue ellipticity ($[\theta]_{MRE}$) at 222 nm, indicating that the protein was nearly devoid of α-helical structure (11). Refolded Apoptin-H_6 also contained little β-sheet structure, which could be deduced from a small positive $[\theta]_{195}$ and a small negative $[\theta]_{216}$ (11). The k2d program for protein secondary structure prediction from CD spectra (12) could not assign any α-helical or β-sheet structure. Although refolded Apoptin-H_6 had little if any secondary structure, it did not adopt a fully random conformation, which would be characterized by a large negative $[\theta]_{190-200}$ (11). It is possible that the flexibility of the polypeptide is restricted because of the high Pro content of Apoptin (12.4%). The negative $[\theta]_{200-210}$ could even suggest the presence of a poly-L-proline helix, although an accompanying small positive $[\theta]_{228}$ was absent (13). Nevertheless, some of Apoptin's Pro residues may adopt a helix-like conformation. The broad negative $[\theta]_{MRE}$ of Apoptin between 210 and 230 nm was reminiscent of CD spectra reported for β-turn- or -hairpin-containing peptides (14, 15). However, the geometry of residues involved in β-turns and -hairpins can vary considerably, making their net contribution to a CD spectrum poorly quantifiable. In general, the CD spectrum of refolded Apoptin-H_6 was very similar to that of proteins that are mostly unstructured (16–19).

The CD spectrum of MBP-Apoptin confirmed these observations, being not significantly different from that of MBP on its own (Fig. 4*B*) (20, 21). First, this result shows that the Apoptin moiety did not perturb the folding of MBP. Second, it demonstrates that Apoptin did not contribute significantly to the secondary structure content of the fusion protein. This is consistent with the very low overall $[\theta]_{MRE}$ of refolded Apoptin-H_6. We conclude that Apoptin displays very little regular secondary structure, but we cannot exclude that some residues adopt a β-strand or -turn conformation.

Intrinsic Fluorescence of Tyr^{95}—Even though Apoptin did not appear to adopt a well defined fold, the Apoptin polypeptide might still display a certain degree of intra- or intermolecular order within the multimeric complex. Because Apoptin-H_6 does not contain any Trp residues, the intrinsic fluorescence of its single Tyr^{95} can act as a structural probe (22, 23). Tyr^{95} is outside the multimerization domain defined by Apoptin's N-terminal residues. The excitation spectrum of Tyr^{95} in refolded Apoptin-H_6 was very similar to that of protonated L-Tyr(-OH), with excitation maxima at 280 and 275 nm, respectively (Fig. 5*A*). However, the fluorescence emission spectrum of Apoptin's Tyr^{95} at pH 6.5 closely resembled that of deprotonated, free tyrosine (L-Tyr(-O^-)) at pH 12 (Fig. 5*B*). This apparent discrepancy can be explained by the effect that excitation has on the pK_a of the Tyr side chain; the pK_a of Tyr(-OH) is near 10 in the ground state but decreases to ~4 upon excitation (24, 25). Because the emission spectrum of refolded Apoptin-H_6 was almost entirely devoid of Tyr(-OH) fluorescence, an efficient proton transfer to a nearby proton-accepting group (Glu, Asp, or His) must have occurred upon excitation of Tyr^{95}. This result indicates that Tyr^{95} was hydrogen bonded. The fluorescence yield of Tyr^{95} was increased by a factor of 4 to 5 relative to fully deprotonated and solvent-exposed L-Tyr(-O^-) (at pH 12), which indicates that Tyr^{95} was at least partially protected from the solvent. The presence of an internal hydrogen bond involving the side chain of Tyr^{95} suggests that at least one region of the Apoptin polypeptide was able to adopt a more ordered conformation.

Apoptin Did Not Bind Zn^{2+} Despite a Putative Zn^{2+}-binding Motif—Apoptin contains a potential metal-binding motif comprised of one His (His^{29}) and three Cys residues (Cys^{30}, Cys^{47}, and Cys^{49}). Although this arrangement does not bear a clear resemblance to any known metal-binding motifs, it is possible that binding of a metal ion by Apoptin influences its secondary structure content or multimerization behavior. The most obvious ligand for this motif would be Zn^{2+}. Including Zn^{2+} in both the expression medium and purification buffers did not affect the expression level, solubility, or net yield of MBP-Apoptin and Apoptin-H_6. Furthermore, the CD spectra of MBP-Apoptin and Apoptin-H_6 were not significantly altered by the presence of Zn^{2+} added either after purification or during expression. The presence of Zn^{2+} affected neither efficiency nor specificity of thrombin digestion of MBP-Apoptin nor the intrinsic fluorescence of refolded Apoptin-H_6. Finally, an assay based on the strong increase in fluorescence upon Zn^{2+} binding of the water-soluble Zn^{2+}-selective chelating dye FluoZin-1 (26) indicated that MBP-Apoptin expressed and purified in the presence of

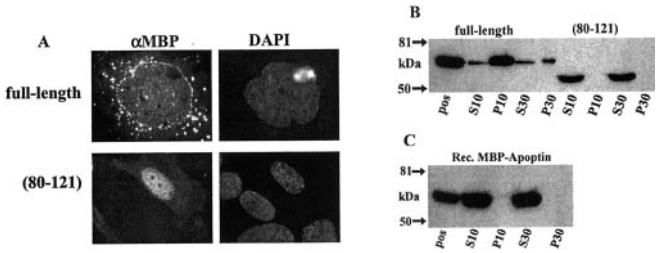

FIG. 6. **Ectopically expressed full-length MBP-Apoptin, but not MBP-Apoptin(80–121), forms distinct globular aggregates in tumor cells.** Immunofluorescence and Western blot analysis of Saos-2 cells, transfected with full-length MBP-Apoptin and MBP-Apoptin(80–121), are shown. *A*, immunofluorescence analysis of Saos-2, transfected with full-length MBP-Apoptin and MBP-Apoptin(80–121). After fixation, the cells were stained with an anti-MBP antibody (*αMBP*). Nuclear morphology is indicated by DAPI staining. Detection with anti-Apoptin αVP3-C produced similar results. *B*, Western blot analysis of supernatant (*S*) and pellets (*P*) of lysed Saos-2 cells, expressing full-length MBP-Apoptin and MBP-Apoptin(80–121). Cell extracts were centrifuged at 10,000 × *g*, yielding S10 and P10, and subsequently at 30,000 × *g*, producing S30 and P30. *Pos* is purified, recombinant MBP-Apoptin. Western blots were stained with αVP3-C. *C*, Western blot analysis of recombinant (*Rec.*) MBP-Apoptin centrifuged at a concentration of 20 μg/ml in lysis buffer alone.

Zn^{2+} contained less than 0.1 mole of Zn^{2+} per mole of protein (data not shown). We conclude that recombinant Apoptin does not form a stable complex with Zn^{2+}.

MBP-Apoptin Expressed in Tumor Cells Exists in an Aggregated State

Having established that recombinant Apoptin protein exists exclusively as a remarkably homogenous and highly stable aggregate *in vitro*, we evaluated the aggregation state of ectopically expressed MBP-Apoptin in human tumor cells (Saos-2). As our data on recombinant MBP-Apoptin(66–121) and MBP-Apoptin(1–69)-H_6 suggested that Apoptin's multimerization domain resided in its N-terminal domain, we expressed MBP-Apoptin(80–121) to compare the appearance of aggregated full-length MBP-Apoptin with that of a truncated, putatively non-aggregating MBP-Apoptin construct.

We inspected the morphological appearance of the two expressed construct in intact cells by immunofluorescence microscopy. Two days after transfection, a time point preceding significant apoptosis induction in this cell type, full-length MBP-Apoptin, was seen to form distinct globular particles in the cytoplasm and nucleus of Saos-2 cells (Fig. 6*A*). Most strikingly, a large proportion of the protein accumulated at the nuclear rim, which may be caused by "congestion" of MBP-Apoptin particles at or in the nuclear pores. In contrast, MBP-Apoptin(80–121) had a much more diffuse appearance and was predominantly located in the nucleus (Fig. 6*A*). We observed essentially the same distribution in HeLa cells (data not shown). These results suggest that full-length MBP-Apoptin becomes aggregated in tumor cells, whereas MBP-Apoptin(80–121) does not. Moreover, these results confirm that MBP itself does not aggregate or contribute to the aggregation of its fusion partner, which is in accordance with the properties of bacterially expressed MBP-Apoptin fusion proteins.

In parallel, we determined the aggregation state of both protein constructs in cell extracts by centrifugation and found that the bulk of the extracted full-length MBP-Apoptin could be pelleted at 10,000 × *g*, indicating that it is or is part of a very dense aggregate (Fig. 6*B*). Moreover, most of the MBP-Apoptin that remained in the supernatant could be pelleted at 30,000 × *g*. Under the same conditions, MBP-Apoptin(80–121) was fully soluble (Fig. 6*A*). Moreover, we verified that recombinant MBP-Apoptin alone did not precipitate upon dilution in lysis buffer (Fig. 6*C*). We assume that the trace amount of full-length MBP-Apoptin remaining in the supernatant after centrifugation at 30,000 × *g* corresponds to newly translated polypeptides that were not yet fully aggregated or had been absorbed by detergent micelles. Taken together with the immunofluorescence data, these results imply that aggregation of Apoptin occurs *in vivo* and that the determinants responsible for aggregation are located in the N-terminal part of the protein.

The Recombinant MBP-Apoptin Protein Complex Is Active as a Multimeric Species

In a separate paper, we show that microinjected recombinant MBP-Apoptin protein induces apoptosis in tumor Saos-2 cells, but not in normal VH10 cells.[3] This observation prompted us to examine the role of aggregation of recombinant MBP-Apoptin in apoptosis induction.

We established that recombinant Apoptin aggregates were not dissolved by cellular factors *in vitro* under physiologically relevant conditions; neither VH10 nor Saos-2 cell lysate affected the size distribution of MBP-Apoptin aggregates in the presence of ATP and Mg^{2+}, as tested by size exclusion chromatography (data not shown). Furthermore, in both Saos-2 and VH10 samples, the characteristic degradation pattern of MBP-Apoptin remained unchanged upon incubation and fractionation. A small amount of untagged Apoptin was present in the starting material, and it remained associated with the intact fusion protein without any changes in ratio (data not shown).

Next, to ensure that MBP-Apoptin aggregates did not dissolve upon microinjection into living cells, we cross-linked the MBP-Apoptin aggregates by brief incubation with 0.05% glutaraldehyde. The majority of these cross-links are expected to be between the MBP moieties if the multimeric fusion protein, as they contain most of the Lys residues. Cross-linked complexes did not contain detectable amounts of smaller oligomers or monomers (Fig. 7*A*). DLS analysis of cross-linked MBP-Apoptin confirmed the presence of a single particle with an R_H of 14.0 ± 1.5 nm. First, this finding demonstrated that cross-linking caused the MBP-Apoptin complex to become more compact. Second, it showed that nearly all cross-linking occurred within complexes, with a negligible number of linkages between different complexes being formed. To follow the fate of MBP-Apoptin complexes upon microinjection, the fluorescent label fluorescein-5-maleimide was attached to Apoptin's single solvent-exposed Cys residue prior to glutaraldehyde cross-linking. When microinjected into the cytoplasm of Saos-2 cells, the fluorescein-labeled, cross-linked MBP-Apoptin was imported into the nucleus and induced the same level of apoptosis within 24 h as non-cross-linked MBP-Apoptin (Fig. 7, *B* and *C*). However, the efficiency of nuclear import of cross-linked MBP-Apoptin appeared to be decreased in comparison to non-cross-linked MBP-Apoptin (data not shown),[3] which may indicate that some of its nuclear localization signals are obscured as a result of glutaraldehyde treatment. In VH10 cells, cross-linked MBP-Apoptin remained in the cytoplasm and did not induce apoptosis (Fig. 7, *B* and *D*). Clearly, covalent cross-linking did not have any significant effect on the activity of microinjected MBP-Apoptin, implying that *in vivo* dissociation of the recombinant Apoptin protein multimers is not required for tumor-specific apoptosis induction.

DISCUSSION

Structure of the Apoptin Complex—We demonstrated with a range of biophysical techniques that recombinant Apoptin protein forms multimeric globules of a distinct size that contain about 30 monomers each. Our scanning force microscopy and electron microscopy studies indicated that Apoptin multimers have a roughly spherical shape. The presence of an 18-residue

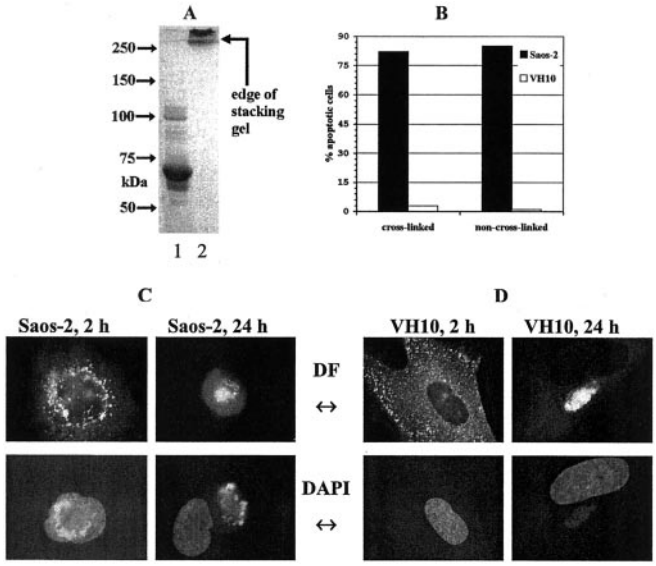

FIG. 7. **Cytoplasmic microinjection of fluorescein-labeled, cross-linked MBP-Apoptin in Saos-2 and VH10 cells.** Irreversible cross-linking of the MBP-Apoptin complex does not affect its nuclear localization or its apoptosis-inducing ability. The Apoptin moiety of MBP-Apoptin was labeled with fluorescein-5-maleimide, and the multimers were cross-linked with 0.05% glutaraldehyde. The incorporation level of fluorescein was near 100%. The fluorescein- and glutaraldehyde-modified MBP-Apoptin was microinjected in Saos-2 and VH10 cells. 100 cells per dish were injected with modified MBP-Apoptin (3 mg/ml, in PBS) and fixed at 2 and 24 h after injection. Injected cells were identifiable by co-injected Lys-fixable rhodamine-dextran. *A*, 7.5% SDS-PAGE analysis of fluorescein-labeled, cross-linked MBP-Apoptin. *1*, non-cross-linked MBP-Apoptin; *2*, cross-linked MBP-Apoptin. *B*, level of apoptosis induction, as determined by DAPI staining. *C*, microinjected Saos-2 cells at 2- and 24-h time points, combined with DAPI staining. *DF*, direct fluorescence of fluorescein-labeled MBP-Apoptin. *D*, microinjected VH10 cells at 2- and 24-h time points, combined with DAPI staining.

linker between MBP and Apoptin in the MBP-Apoptin fusion protein increased its hydrodynamic radius, leading to an overestimation of its molecular mass. When MBP-Apoptin complexes were cross-linked with glutaraldehyde, they became more compact as judged by DLS, presumably because the MBP moieties became firmly attached to each other and to the body of the Apoptin core. On the basis of its hydrodynamic radius, the theoretical molecular mass of the cross-linked MBP-Apoptin complex is 1.6 MDa, corresponding to 30 monomeric subunits. This is fully consistent with the monomer content of refolded Apoptin-H_6 we observed.

CD spectroscopy indicated that Apoptin protein multimers contain little if any secondary structure, which may reflect a lack of internal ordering. This result raises the question of how a seemingly disordered Apoptin polypeptide can assemble into a biologically active and homogenous protein multimer. We hypothesize that Apoptin multimers consist of only a limited number of monomer conformations. Our experimental results on recombinant Apoptin protein support such an idea. First, we demonstrated that Apoptin's Tyr^{95} forms a stable hydrogen bond, which implies that there is at least some internal structure. Second, the CD spectrum of refolded Apoptin-H_6 was clearly different from that of a true random coil polypeptide, indicating that its conformational freedom was restricted (11). If Apoptin multimers present an at least partially ordered surface, this characteristic would allow them to interact selectively with cellular factors. Such an interaction could give rise to a particular biological effect, namely the induction of apoptosis in a tumor-specific manner. Furthermore, it could be that small domains of the Apoptin multimer become ordered once recognized by cellular factors. There are precedents for such behavior; for example, high mobility group proteins specifically recognize DNA, yet in the absence of DNA do not adopt a regular conformation (27).

According to secondary structure prediction, Apoptin might fold as an anti-parallel β-sheet between Glu^{32} and Leu^{46} with Ala^{38} and Gly^{39} oriented in a β-turn or -hairpin. The CD spectrum of refolded Apoptin-H_6 is consistent with such a short anti-parallel β-sheet. In this motif (^{29}HCREIRIGIAGITITLSLCGC^{49}), small, mostly hydrophilic residues alternate with seven Leu and Ile side chains. In addition, this motif is flanked by a potential metal-binding site (His^{29}, Cys^{30}, Cys^{47}, and Cys^{49}). However, we showed that this configuration of Cys and His residues did not constitute a Zn^{2+}-binding site in recombinant Apoptin. If this sequence indeed adopts a β-hairpin-type conformation, the large hydrophobic residues would all protrude from one of the faces of the hairpin, whereas the hydrophilic residues would protrude from the other. Such an amphipathic motif could well be essential for the multimerization properties of Apoptin, perhaps by allowing the Leu and Ile residues of neighboring Apoptin monomers to interlock. Our observation that the presence of OG caused MBP-Apoptin to precipitate does suggest that the multimerization of Apoptin is, at least to an extent, based on hydrophobic interactions. It may be that OG is more effective than CHAPSO and Triton in disrupting Apoptin multimers because of its small size and high micelle concentration (~9 mM or ~0.3%), allowing it to penetrate the Apoptin core of MBP-Apoptin.

The Leu/Ile clustering of the potential amphipathic β-hairpin is reminiscent of a Rev- or PKIα–like nuclear export signal (NES) (28). Although the NES sequences of PKIα and of p53 have been reported to adopt an amphipathic α-helical conformation (29, 30), CD spectroscopy showed that refolded Apoptin-H_6 did not contain any α-helical regions. If indeed the isoleucines and leucines of the putative NES of Apoptin are part of its multimerization motif, these residues would, because of their hydrophobic nature, be largely buried within the multimer. Thus obscured, Apoptin's putative NES would be likely to have reduced activity.

Activity of the Apoptin Complex—We established that ectopically expressed, full-length MBP-Apoptin was aggregated in live tumor cells, whereas truncated MBP-Apoptin(80–121) was not. This difference in aggregation state was consistent with our findings on recombinant MBP-Apoptin and truncated versions thereof. Moreover, the distribution of ectopically expressed MBP-Apoptin, including its accumulation at the nuclear envelope, was similar to that of the recombinant protein following microinjection.[3] Furthermore, the size of the aggregates formed by full-length MBP-Apoptin *in vivo* was remarkably regular. Such homogeneity is strongly reminiscent of the narrow size distribution of bacterially expressed MBP-Apoptin. However, ectopically expressed MBP-Apoptin was contained in an aggregate particle that was denser than the recombinant Apoptin protein multimer. Therefore, it is likely that Apoptin expressed *in vivo* forms a larger aggregate or co-aggregates with other cellular proteins.

Our results suggest that aggregation of Apoptin *in vivo* does not preclude induction of apoptosis, which would imply that Apoptin does not have to be a properly folded molecule to be active. Moreover, as most if not all ectopically expressed MBP-Apoptin was found to be aggregated, it is very likely that this aggregated state represents the physiological form of Apoptin in tumor cells. Alternatively, it is possible that the protein undergoes a transition between a folded and an unfolded state *in vivo* upon binding to some cellular factor. We expect that an inducible Apoptin expression system in human tumor cells will

allow us to evaluate the molecular mass distribution of ectopically expressed Apoptin in more detail.

Based on the findings reported here, we hypothesize that the multimeric state is the functional form of recombinant MBP-Apoptin, which we propose to be analogous to the aggregated state of ectopically expressed MBP-Apoptin. First, cell lysates could not bring about the efficient dissolution of the Apoptin multimers into monomers or smaller oligomers. Second, chemical cross-linking of MBP-Apoptin did not significantly affect its subcellular localization and apoptosis-inducing ability in human tumor cells. Moreover, cross-linked Apoptin protein multimers did not kill normal cells. Taken together, these results clearly demonstrate that Apoptin does not have to adopt a monomeric form to be active as a tumor-specific apoptosis-inducer. Nevertheless, these results do not formally rule out the possibility that Apoptin might exist as a monomer *in vivo*. However, it should be noted that both MBP-Apoptin and Apoptin-H_6 multimers were found to be remarkably stable. They could not be dissolved under native conditions *in vitro*, suggesting that no significant amounts of monomeric Apoptin were ever released. Even under denaturing conditions (8 M urea or 6 M guanidinium hydrochloride), the interactions between individual Apoptin proteins were only partially abolished (data not shown). Clearly, the driving force behind multimer formation is dominant both in the intracellular environment of *E. coli* and while Apoptin-H_6 was tethered to Ni^{2+}-chelating resin under refolding conditions, which suggests that multimerization is probably the fate of a significant fraction of *in vivo* expressed Apoptin, as well. In all, we conclude that aggregated, or multimeric, recombinant Apoptin protein contains the essential features that allow Apoptin, expressed *in vivo*, to induce apoptosis in a tumor-specific manner. Moreover, we conclude that the lack of secondary structure in recombinant Apoptin protein is likely to reflect, at least to some extent, the intrinsically disordered nature of Apoptin.

There are many examples of proteins that can undergo controlled denaturation/aggregation or polymerization *in vitro* (31–33). In general, controlled aggregation occurs under conditions that stabilize a particular folding intermediate. The disruption of a folding pathway *in vivo* that leads to the accumulation of such intermediates in intracellular aggregates is linked to several pathological processes. Hence, evolution of protein secondary and tertiary structure is thought to be aimed, at least in part, on bypassing such kinetic folding "sinks" of partially folded polypeptides (34). A well documented example of a pathogenic, aggregation-prone protein is huntingtin, the pathogenic effect of which is characterized by the formation of intranuclear aggregates of N-terminal huntingtin fragments, an event that is directly linked to apoptosis induction (35). An example where protein aggregation seems to represent "gain-of-function" is the human milk protein α-lactalbumin, which forms partially unfolded oligomers that are imported into the nucleus of tumor and differentiating cells, whereas the monomeric form is not. Nuclear import of oligomeric α-lactalbumin was accompanied by induction of apoptosis (36, 37). It has been suggested that the presence of globular aggregates of misfolded protein in the cell may lead to cell death if these aggregates are efficient nucleation sites for fibrous amyloid formation (33). However, the globular aggregates of recombinant Apoptin did not form recognizable fibrous amyloid deposits when microinjected into live cells,[3] and such amyloid formation by Apoptin was also not observed *in vitro* in the current study. Therefore, the mechanism of apoptosis induction by Apoptin is clearly different. Moreover, apoptosis induction by recombinant Apoptin multimers is not a general cytotoxic effect, as Apoptin does not appear to elicit any harmful effects when introduced into several different normal primary human cells.[3] Apoptin will exert its pro-apoptotic function only when a cell has entered the pathway that leads to a transformed state (38). In that respect, Apoptin clearly differs from proteins that give rise to aggregation-linked diseases (39).

Apoptin is a viral protein encoded by chicken anemia virus. The virus has a minimal single-stranded DNA genome, and Apoptin's gene fully overlaps with that of the VP2 protein, albeit with a shift in frame (40). One possible function of Apoptin in the replication cycle of CAV is to induce apoptosis of infected chicken thymocytes to release them from the host cell once the viral particles have matured. Transmission of CAV may be enhanced when the virus is encased in or associated with apoptotic bodies, analogous to adenoviral vectors (41). In such a process, the potential co-transmission of Apoptin globules, together with infectious viral particles, may also have a biological function. In this respect it is striking that Apoptin forms a globular particle roughly the size of a virus, so it may have an evolutionary relationship with a viral coat protein. The requirement of a compact genome in CAV has impelled the Apoptin gene to fully overlap with that of VP2 in the viral genome. The obvious price of this compactness is that the sequences of both genes are more strongly constrained. However, if a protein's function requires it merely to aggregate, rather than to adopt a well defined quaternary conformation, the constraints on its sequence will be less stringent.

It is well possible that Apoptin's original function has demanded its multimerization, which it may have achieved through random aggregation as outlined above, rather than through the formation of a specific quaternary structure. If so, Apoptin provides an example of a novel route for the evolution of protein function. There are several possible explanations why the multimerization of Apoptin may be essential for its biological function; *e.g.* aggregation may stabilize Apoptin, which in its ill-defined monomeric form may be readily degradable, or the formation of globular multimers may result in cooperative binding of Apoptin moieties to certain large ligands or molecular complexes (DNA, RNA, chromatin, nuclear pores, etc.). Obviously these possibilities do not exclude one another, underscoring the likeliness that in the case of Apoptin the classical structure/function paradigm translates as an aggregation/function paradigm.

Acknowledgments—We thank Hans van der Meulen (Leiden University Medical Center) for performing electron microscopic analysis and Remus Thei Dame (Molecular Genetics, Leiden University) for performing scanning force microscopic analysis of MBP-Apoptin. Furthermore, we extend our gratitude to Fred Wassenaar (Leiden University Medical Center) for the donation of the vector pMalTB. We are also grateful to Klaas Kooistra (Leadd B.V.) for culturing VH10 and Saos-2 cells.

REFERENCES

1. Noteborn, M. H., Todd, D., Verschueren, C., de Gauw, H., Curran, W., Veldkamp, S., Douglas, A., McNulty, M., van der Eb, A., and Koch, G. (1994) *J. Virol.* **68,** 346–351
2. Danen-van Oorschot, A. A., Fischer, D., Grimbergen, J., Klein, B., Zhuang, S.-M., Falkenburg, J., Backendorf, C., Quax, P., van der Eb, A., and Noteborn, M. (1997) *Proc. Natl. Acad. Sci. U. S. A.* **94,** 5843–5847
3. Zhuang, S.-M., Landegent, J. E., Verschueren, C. A., Falkenburg, J. F., van Ormondt, H., van der Eb, A. J., and Noteborn, M. H. (1995) *Leukemia* **9,** Suppl. 1, 118–120
4. Kapust, R., and Waugh, D. (1999) *Protein Sci.* **8,** 1668–1674
5. Wang, C., Castro, A., Wilkes, D., and Altenberg, G. (1999) *Biochem. J.* **338,** 77–81
6. Stempfer, G., Holl-Neugebauer, B., and Rudolph, R. (1995) *Nature Biotechnol.* **14,** 329–334
7. Lee, G. (1989) *J. Cell Sci.* **94,** 443–447
8. Minascheck, G., Bereiter-Hahn, J., and Bertholdt, G. (1989) *Exp. Cell Res.* **183,** 434–442
9. Danen-van Oorschot, A., van der Eb, A., and Noteborn, M. (2000) *J. Virol.* **74,** 7072–7078
10. Riddles, P. W., Blakeley, R. L., and Zerner, B. (1983) *Methods Enzymol.* **91,** 49–60
11. Rodger, A., and Norden, B. (1997) *Circular Dichroism and Linear Dichroism. Oxford Chemistry Masters* (Compton, R. G., Davies, S. G., and Evans, J.,

eds), pp. 20–22, Oxford University Press, Oxford
12. Andrade, M., Chacon, P., Merelo, J., and Moran, F. (1993) *Protein Eng.* **6,** 383–390
13. Kelly, M., Chellgren, B., Rucker, A., Troutman, J., Fried, M., Miller, A., and Creamer, T. (2001) *Biochemistry* **40,** 14736–14383
14. Ramirez-Alvarado, M., Blanco, F., Niemann, H., and Serrano, L. (1997) *J. Mol. Biol.* **273,** 898–912
15. Griffiths-Jones, S., Maynard, A., and Searle, M. (1999) *J. Mol. Biol.* **292,** 1051–1069
16. Kriwacki, R., Hengst, L., Tennant, L., Reed, S., and Wright, P. (1996) *Proc. Natl. Acad. Sci. U. S. A.* **93,** 11504–11509
17. Cregut, D., and Serrano, L. (1999) *Protein Sci.* **8,** 271–282
18. McCutchen-Maloney, S., Matsuda, K., Shimbara, N., Binns, D., Tanaka, K., Slaughter, C., and DeMartino, G. (2000) *J. Biol. Chem.* **275,** 18557–18565
19. Adkins, J., and Lumb, K. (2002) *Proteins Struct. Funct. Genet.* **46,** 1–7
20. Ganesh, C., Shah, A., Swaminathan, C., Surolia, A., and Varadarajan, R. (1997) *Biochemistry* **36,** 5020–5028
21. Fischer, M., Corringer, P., Schott, K., Bacher, A., and Changeux, J. (2001) *Proc. Natl. Acad. Sci. U. S. A.* **98,** 3567–3570
22. Härd, T., Hsu, V., Sayre, M., Geiduschek, E., Appelt, K., and Kearns, D. (1989) *Biochemistry* **28,** 396–406
23. Ferreira, S., Stella, L., and Gratton, E. (1994) *Biophys. J.* **66,** 1185–1196
24. Szabo, A., Lynn, K., Krajcarski, D., and Rayner, D. (1978) *FEBS Lett.* **94,** 249–252
25. O'Neill, J., and Hofmann, T. (1987) *Biochem. J.* **243,** 611–615
26. Gee, K., Zhou, Z., Qian, W., and Kennedy, R. (2002) *J. Am Chem. Soc.* **124,** 776–778
27. Reeves, R. (2001) *Gene* **277,** 63–81
28. Elfgang, C., Rosorius, O., Hofer, L., Jaksche, H., Hauber, J., and Bevec, D. (1999) *Proc. Natl. Acad. Sci. U. S. A.* **96,** 6229–6234
29. Hauer, J., Barthe, P., Taylor, S., Parello, J., and Padilla, A. (1999) *Protein Sci.* **8,** 545–553
30. Lee, W., Harvey, T., Yin, Y., Yau, P., Litchfield, D., and Arrowsmith, C. (1994) *Nat. Struct. Biol.* **1,** 877–890
31. Roefs, P., and de Kruif, K. (1994) *Eur. J. Biochem.* **226,** 883–889
32. Chiti, F., Webster, P., Taddei, N., Clark, A., Stefani, M., Ramponi, G., and Dobson, C. (1999) *Proc. Natl. Acad. Sci. U. S. A.* **96,** 3590–3594
33. Buccianti, M., Giannoni, E., Chiti, F., Baroni, F., Formigli, L., Zurdo, J., Taddei, N., Ramponi, G., Dobson, C., and Stefani, M. (2002) *Nature* **416,** 507–511
34. Lansbury, P. (1999) *Proc. Natl. Acad. Sci. U. S. A.* **96,** 3342–3344
35. Li, S., Lam, S., Cheng, A., and Li, X. (2000) *Hum. Mol. Genet.* **9,** 2859–2867
36. Svennson, M., Sabbharwa, H., Hakansson, A., Mossberg, A.-K., Lipniunas, P., Leffler, H., Svanborg, C., and Linse, S. (1999) *J. Biol. Chem.* **274,** 6388–6396
37. Svensson, M., Hakansson, A., Mossberg, A.-K., Linse, S., and Svanborg, C. (2000) *Proc. Natl. Acad. Sci. U. S. A.* **97,** 4221–4226
38. Noteborn, M., Zhang, Y., and van der Eb, A. (1998) *Mutat. Res.* **400,** 447–255
39. Dobson, C. (2001) *Philos. Trans. R. Soc. Lond.-Biol. Sci.* **356,** 133–145
40. Noteborn, M., de Boer, G., van Roozelaar, D., Karreman, C., Kranenburg, O., Vos, J., Jeurissen, S., Hoeben, R., Zantema, A., Koch, G., van Ormondt, H., and van der Eb, A. (1991) *J. Virol.* **65,** 3131–3139
41. Mi, J., Li, Z., Ni, S., Steinwaerder, D., and Lieber, A. (2001) *Hum. Gene Ther.* **12,** 1343–1352

Apoptin Induces Tumor-specific Apoptosis as a Globular Multimer

Sirik R. Leliveld, Ying-Hui Zhang, Jennifer L. Rohn, Mathieu H. M. Noteborn and Jan Pieter Abrahams

J. Biol. Chem. 2003, 278:9042-9051.
doi: 10.1074/jbc.M210803200 originally published online December 19, 2002
